

pH-sensitive liposomes as a carrier for oligonucleotides: a physico-chemical study of the interaction between DOPE and a 15-mer oligonucleotide in quasi-anhydrous samples

Mônica Cristina De Oliveira ^{a,b}, Elias Fattal ^a, Patrick Couvreur ^a, Pierre Lesieur ^c,
Claudie Bourgaux ^c, Michel Ollivon ^a, Catherine Dubernet ^{a,*}

^a URA CNRS 1218, Physico-chimie-Pharmacotechnie-Biopharmacie, Université Paris 11, Centre d'Etudes Pharmaceutiques,
5 rue Jean Baptiste Clément, 92296 Châtenay-Malabry Cedex, France

^b Faculdade de Farmácia da Universidade Federal de Minas Gerais, Avenida Olegário Maciel, 2360, 30180-112 Belo Horizonte/MG, Brazil

^c LURE, Laboratoire pour l'Utilisation du Rayonnement Electromagnétique, Université Paris Sud, 91405 Orsay, France

Received 7 January 1998; revised 6 April 1998; accepted 16 April 1998

Abstract

pH-sensitive liposomes made of dioleoylphosphatidylethanolamine (DOPE)/oleic acid (OA)/cholesterol (CHOL) mixtures were shown to be very promising carriers for oligonucleotides (ON). However, it appeared necessary to clarify the structural consequence of the interactions of ON with the liposome, and especially on DOPE, the lipid responsible for the pH sensitivity. The present study was carried out by differential scanning calorimetry and X-ray diffraction, at low hydration. In such a case, DOPE generally adopt a hexagonal phase. It could be shown that ON increased DOPE transition temperature and increased v/a , as a result of electrostatic interactions between ON and DOPE headgroups. OA was found to have exactly opposite effects, its presence between DOPE molecules inhibiting the formation of hydrogen bonds. The presence of both ON and OA allowed the system to organize in a lamellar phase below the solid/liquid transition, whereas above this temperature ON preferably interacted with DOPE in a hexagonal phase and led OA to separate. © 1998 Elsevier Science B.V. All rights reserved.

Keywords: pH sensitive liposome; Antisense oligonucleotide; Dioleoylphosphatidylethanolamine; Oleic acid; Differential scanning calorimetry; X-Ray diffraction

1. Introduction

Liposomes are generally taken up by the cells through an endocytosis process which leads to the release of the encapsulated drug in the lysosomes. This compartment, particularly rich in enzymes,

may, however, be aggressive against sensitive drugs such as proteins, or nucleic acids. To circumvent this problem, it is necessary to deliver the encapsulated drug into the cell cytoplasm before the formation of phagolysosomes. pH-sensitive liposomes, which have been designed for this purpose, can be considered efficient cytoplasmic delivery systems for a variety of drugs [1–7].

The concept of pH-sensitive liposomes is based on the destabilization of liposomal membranes in an acidic environment, such as the endosomes, with a

* Corresponding author. Fax: +33 (1) 46619334;
E-mail: catherine.dubernet@cep.u-psud.fr

subsequent release of trapped molecules. The construction of pH-sensitive liposomes takes advantage of the polymorphic phase behaviour of unsaturated phosphatidylethanolamine (PE) which forms inverted hexagonal phase (HII) rather than bilayers under physiological conditions of pH and temperature. Liposome stabilization into bilayers at neutral pH can be achieved using several titratable acid lipids, such as cholesterylhemisuccinate (CHEMS) [8], *N*-palmitoylhomocysteine (PHC) [9], oleic acid (OA) [10] or diacylsuccinylglycerols [11], which are negatively charged at neutral pH. These lipids, homogeneously distributed among PE molecules, provide electrostatic repulsions which decrease PE intermolecular interactions, thus preventing HII phase formation under physiological conditions. The protonation of these acid lipids in the acidic endosomal compartment neutralizes their negative charges, and the vesicles become destabilized as the PE component reverts to HII phase. It has been evidenced that the formation of this non-bilayer phase (HII) plays an important role in the leakage of liposome content [12].

As oligonucleotides are very sensitive to degradation in biological medium, especially by nucleases, it is particularly interesting to deliver them encapsulated within pH-sensitive liposomes [13–15]. Biological results, in terms of inhibition of the Friend retrovirus, confirmed the superiority of pH-sensitive liposomes against conventional ones. However, in some conditions it was suspected that oligonucleotides might interfere with the organization of the lipids, as attested by scanning electron microscopy [14]. If oligonucleotide molecules modify the L α -HII phase transition, the pH sensitivity of the liposomes might be altered.

This paper investigates the effects of the addition of oligonucleotide molecules on the phase behaviour of dioleoylphosphatidylethanolamine (DOPE), in the presence or absence of OA and cholesterol (CHOL). Thermal behaviour of DOPE was examined by differential scanning calorimetry (DSC), and X-ray diffraction measurements recorded at different temperatures were used to characterize the phases involved. Small angle (SAXS) and wide angle (WAXS) X-ray scatterings were both performed, but only SAXS diffraction patterns gave remarkable information and hence are discussed in this paper. The study was

performed with quasi-anhydrous preparations, in order to be able to identify the lipid compartment at low temperatures in the absence of ice formation. Such a study represents a prerequisite for the examination of more diluted systems since the presence (or the absence) of interactions between oligonucleotide molecules and the lipid components of pH-sensitive liposomes in such concentrated and confined systems will shed some light on the behaviour of more diluted preparations.

2. Materials and methods

2.1. Materials

1,2-Dioleoyl-*sn*-glycero-3-phosphatidylethanolamine (DOPE), OA and CHOL as well as ethylenediaminetetraacetic acid (EDTA) and tris(hydroxymethyl)aminomethane (Tris) were purchased from Sigma (St. Louis, MO, USA). Lipids were used without further purification. The 15-mer phosphorylated oligonucleotide (ON), 5'-TGAACACGCCATGTC-3' (complementary sequence to the region of the start codon AUG of Friend virus env gene), was obtained from Eurogentec (France).

2.2. Sample preparation

DOPE, OA and CHOL were dissolved in chloroform and mixed in proportion to achieve the desired molar fractions (1:0:0, 1:0.4:0, 1:1.3:0, 1:2.4:0 and 1:1.3:0.4). The resulting mixtures were then evaporated to dryness under reduced pressure. The dry residue was hydrated at 30°C with 50 mM Tris containing 5 mM EDTA (pH 8.5). Liposomes were then calibrated by successive extrusion through 0.4 and 0.2 mm polycarbonate membranes, except for pure DOPE liposomes that were simply hydrated at 4°C, below the lamellar to hexagonal phase transition temperature. When needed, oligonucleotide was added at an ON/DOPE molar ratio of 0.02. Liposomes were then submitted to three cycles of freeze-thawing. Non-entrapped oligonucleotide was eliminated by ultracentrifugation (3 times, 150 000 \times g, 40 min each, 4°C). Samples purified in such a way, which displayed an ON/DOPE molar ratio 10 times lower than unpurified preparations, were then

lyophilized. Aliquots containing 2–5 mg of DOPE were introduced in pre-weighed DSC aluminium pans and hydrated over saturated solution of $\text{Mg}(\text{NO}_3)_2$, at 4°C (58.8% relative humidity), until constant weight. The water weight fraction for the different samples ranged between 0.064 and 0.094 (Table 1). At equilibrium, the different pans were weighed, sealed and analysed by DSC. For X-ray diffraction analysis, the hydrated samples were transferred to a X-ray capillary.

2.3. Differential scanning calorimetry

Calorimetric analyses were performed on a Perkin-Elmer DSC 7 instrument (Norwalk, CT, USA) at a heating rate of 2.5°C/min. Indium and *n*-decane were used for temperature and enthalpy calibration. Precisely weighted samples (corresponding to 2–5 mg DOPE) were scanned from –45 to 110°C. Data acquisition and analysis were performed on a micro-computer using a DSC 7 Isothermal Software Kit provided by Perkin-Elmer. The transition temperatures were defined by the position of the peak maximum.

2.4. X-Ray diffraction

As mentioned above, the X-ray specimens were added to thin glass capillaries (GLAS, Muller, Berlin, Germany) (0.01 mm wall thickness, diameter < 1.5 mm), by means of centrifugation (5500 rpm). Samples were kept under argon and the capillaries were sealed with a drop of melted paraffin, and maintained at 4°C until analysis. Laboratory-made sample holders allowing X-ray diffraction examination in the –30°C/+130°C temperature range were used. Sample temperature was measured by a thin thermocouple placed next to the capillary on the same axis. The thermocouple was placed in a closed loop together with a temperature controller (Eurotherm 902P) and sample holder heater. This set up allowed 0.1°C accuracy. The D22 and D24 benches of the DCI synchrotron of LURE were used alternatively ($\lambda = 1.377 \text{ \AA}$ and 1.489 \AA , respectively) [16]. Diffraction patterns were obtained after thermal equilibration and X-ray exposure of 200 s. The structural dimensions of each phase observed were calculated from X-ray diffraction measurements as explained in Fig. 6, considering as d_{lam} or d_{hex} the diffraction line of first order.

Table 1

Structural parameters of DOPE^a and DOPE based mixtures as a function of temperature and composition (meaning of parameters is shown Fig. 6)

Sample	Water weight fraction	Temperature (°C)	$d_{\text{hex/cub}}$ (Å)	R_w (Å)	d_l (Å)	d_m (Å)	d_{lam} (Å)	d_b (Å)	d_w (Å)
DOPE	0.087	–25.0	58.05	10.38	46.27	56.64	–	–	–
DOPE	0.087	–6.5	56.15	10.04	44.75	54.75	–	–	–
DOPE+ON ^b	0.094	–28.0	56.15	10.43	43.98	54.01	–	–	–
DOPE+ON ^b	0.094	–0.6	51.53	9.58	40.34	49.54	–	–	–
DOPE-OA ^c	0.075	–28.0	61.24	10.17	50.37	61.31	–	–	–
DOPE-OA ^c	0.075	–5.4	57.80	9.59	47.56	57.88	–	–	–
DOPE-OA+ON ^c	0.064	–28.0	–	–	–	–	53.13	49.73	3.40
DOPE-OA+ON ^c	0.064	–6.5	64.24	9.85	54.48	66.06	–	–	–
DOPE-OA-CHOL ^d	0.084	–6.0	(66.14) ^e	–	–	–	–	–	–
DOPE-OA-CHOL ^d	0.084	43.0	54.17	9.52	43.51	53.18	–	–	–
DOPE-OA-CHOL+ON ^{b,d}	0.080	–29.0	–	–	–	–	50.27	46.24	4.02
DOPE-OA-CHOL+ON ^{b,d}	0.080	–15.0	–	–	–	–	48.33	44.46	3.87

^aVolume of one molecule of anhydrous DOPE is equivalent to 1228 Å³ [18].

^bThese samples refer to purified preparations (low oligonucleotide concentration).

^cDOPE/OA molar ratio equivalent to 1.0:1.3.

^dDOPE/OA/CHOL molar ratio equivalent to 1.0:1.3:0.4.

^eNumber in parentheses concerns cubic phase.

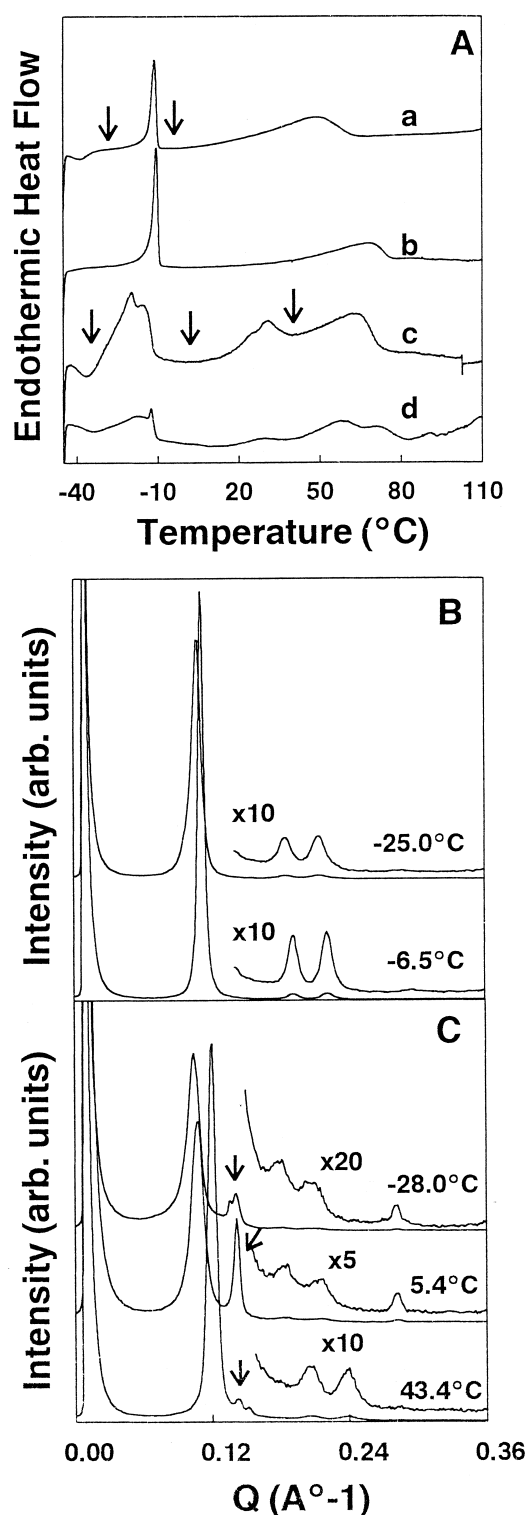


Fig. 1. Effect of increasing amounts of OA on the phase behaviour of DOPE (A) and corresponding X-ray patterns of DOPE (B) and OA-DOPE system at a molar ratio equal to 1.3 (C). The calorimetric thermograms were recorded in the absence (a) and in the presence of OA at OA/DOPE ratios of (b) 0.4, (c) 1.3 and (d) 2.4. Arrows show the temperatures at which X-ray patterns were obtained.

3. Results

3.1. DOPE-OA mixtures

DOPE-OA mixtures in the range of 0–2.4 OA/DOPE molar ratio were first submitted to DSC analysis (Fig. 1A). DOPE, in the presence of buffer salts, showed a transition temperature centred at -11°C . For an OA/DOPE molar ratio of 0.4, no modification of the transition temperature was observed. However, the addition of OA in higher proportions decreased the transition temperature, promoted the splitting of the peak, and gave birth to an endotherm around 30°C . This slight endotherm was attributed to the solid-liquid transition of OA itself, as indicated by the control analysis (OA in the presence of buffer salts) (data not shown). The large endotherm observed between 40 and 78°C refers to the hydrated buffer salts themselves as determined by DSC recordings of control buffer salts (data not shown). It is noteworthy that the addition of OA to DOPE samples increases the temperature of this last endothermic peak. Diffraction patterns of DOPE, at -25 and -6.5°C , showed X-ray spacings in the ratios of 1 , $1/\sqrt{3}$, $1/\sqrt{4}$, which characterize the presence of a hexagonal phase (Fig. 1B). In the presence of OA at a molar ratio of 1.3, and at temperatures of -28 , 5.4 and 43.4°C , X-ray spacings were also found in the ratios of 1 , $1/\sqrt{3}$, $1/\sqrt{4}$, indicating the existence of a hexagonal phase of DOPE (Fig. 1C). Moreover, one line was identified at 5.4°C (about 44.6 \AA) and two reflections at -28 (about 46.3 and 44.6 \AA) and 43.4°C (about 43.6 and 41.8 \AA), attributed to OA phase (arrows in Fig. 1C).

3.2. DOPE-OA-CHOL mixtures

The influence of the addition of cholesterol on DOPE-OA mixtures was determined using a fixed added amount (15 mol%). It led to a decrease of

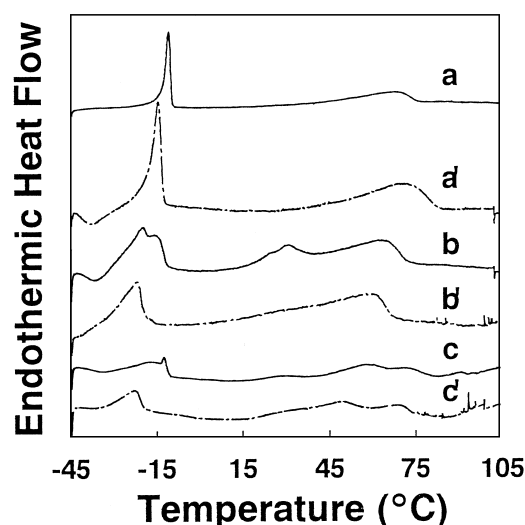


Fig. 2. Influence of cholesterol (15 mol%) on the phase transition of different mixtures of DOPE and OA. Calorimetric traces are shown in the absence of cholesterol (a,b,c) and in its presence (a',b',c') in the case of OA/DOPE molar ratios of 0.4 (a,a'), 1.3 (b,b') and 2.4 (c,c').

the lower transition temperature and abolished the splitting of the peak in the case of OA/DOPE molar ratios equal to 1.3 and 2.4 (Fig. 2). On the other hand, in the case of lower OA/DOPE molar ratio (0.4), addition of cholesterol slightly increased the width of the transition peak of DOPE. Fig. 2 also shows that the introduction of cholesterol in the OA-DOPE mixture, 1.3 molar ratio, abolished the endotherm around 30°C, and broadened this transition in the case of 2.4 OA/DOPE molar ratio.

3.3. DOPE-oligonucleotide mixtures

Fig. 3A depicts the influence of two oligonucleotide concentrations on the phase behaviour of DOPE. Preparations submitted to the purification step by ultracentrifugation showed an endothermic transition at -7°C , which was increased by 4°C in comparison with DOPE phase transition. Such purified samples can be considered as low concentrated in ON (DOPE:ON 1:0.002). In the case of unpurified samples (DOPE:ON 1:0.02), the shift of this peak was even more pronounced ($6\text{--}7^{\circ}\text{C}$). As previously observed with OA, the addition of ON molecules to DOPE samples (DOPE:ON 1:0.002) leads to the shift of the peak corresponding to the buffer salts towards higher temperatures (around 70°C). Con-

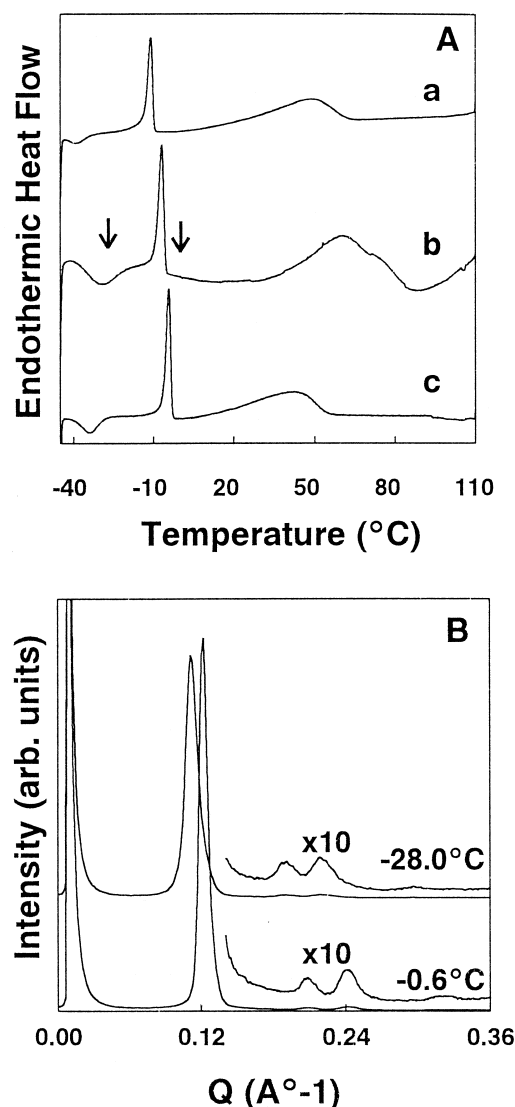


Fig. 3. Effect of two concentrations of ON on the phase behaviour of DOPE (A) and corresponding X-ray patterns of a purified DOPE-ON preparation (B). The calorimetric traces were recorded in the absence of ON (a), in the case of a low ON concentration (purified liposomes) (b) and a high ON concentration (unpurified liposomes) (c). Arrows show the temperatures at which X-ray patterns were obtained.

cerning X-ray analysis and as described above, hexagonal phase was found in DOPE samples at both -25 and -6.5°C (Fig. 1B). In the case of a low concentrated oligonucleotide-DOPE mixture, the small-angle reflections, at -28 and -0.6°C , were also in the ratio of 1, $1/\sqrt{3}$, $1/\sqrt{4}$ and demonstrated therefore the existence of a hexagonal phase (Fig. 3B).

3.4. DOPE-OA-ON mixtures

The effect of ON (low concentration) on the thermal events of DOPE:OA 1:1.3 is shown in Fig. 4A. These ratios were chosen with regard to the final lipids to ON concentrations in pH-sensitive liposomes. The main transition temperature appeared

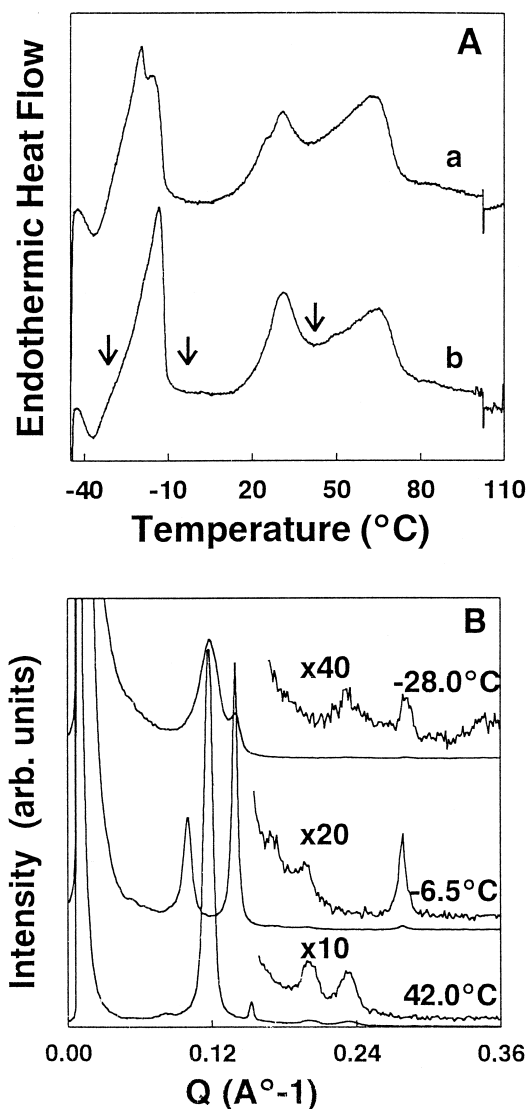


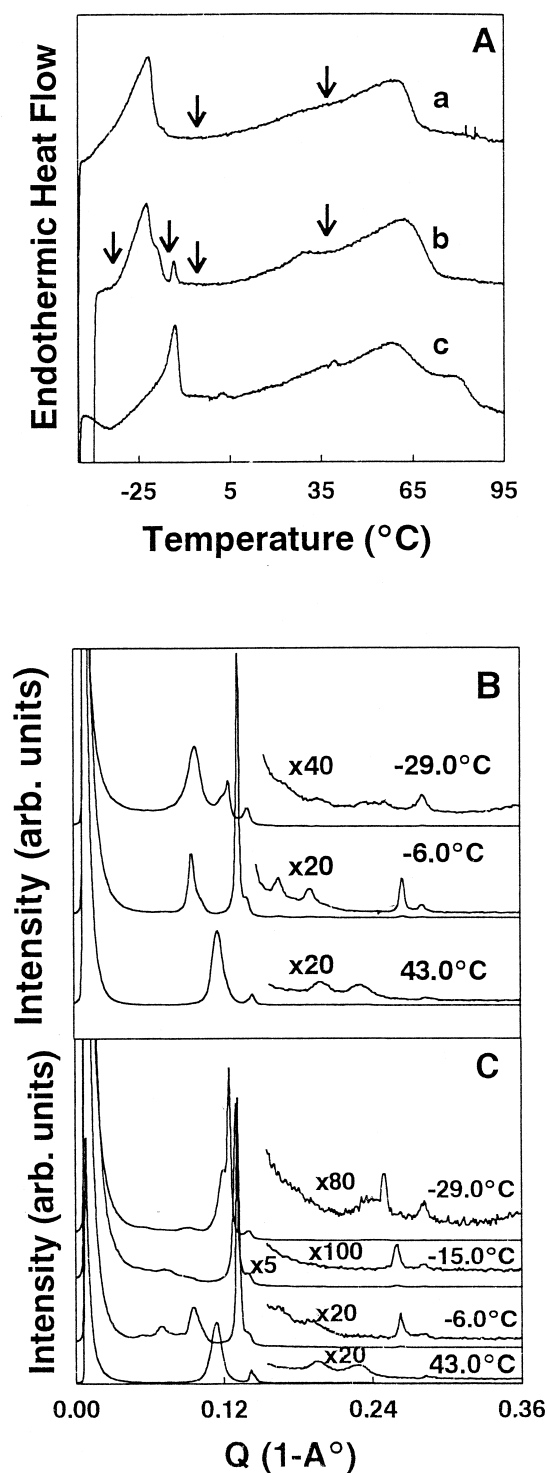
Fig. 4. Thermal phase behaviour of an oligonucleotide-containing OA-DOPE system (1.3 molar ratio) (A). The calorimetric traces are shown in the absence (a) and in the presence of a low ON concentration (0.002 ON/DOPE molar ratio) (b). Arrows show the temperatures at which X-ray patterns were obtained. X-Ray diffraction lines (B) are those of an OA-DOPE system (1.3 molar ratio) containing oligonucleotide (0.002 ON/DOPE molar ratio).

shifted upwards in the presence of oligonucleotides and the splitting of the peak seemed to be abolished. Concomitantly, the enthalpy of the endotherm around 30°C was increased. X-Ray measurements at -28°C showed the presence of both hexagonal and lamellar phases in the OA-DOPE system (1.3:1 molar ratio), corresponding to DOPE and OA, respectively, as described above (Fig. 1C). In contrast, for the OA-DOPE-ON-containing system (Fig. 4B), two series of two X-ray line spacings in the ratios of the unit-cell dimension, d_{lam} , 1/1, 1/2, were observed at -28°C. At -6.5°C, however, reflections were different, in the ratios of 1, 1/√3, 1/√4 and 1/1, 1/2, indicating the coexistence of hexagonal and lamellar phases. Lastly, at 42°C, the X-ray patterns showed line spacings in the ratios of 1, 1/√3, 1/√4 and a shorter reflection at 41.1 Å (Fig. 4B). Thus, X-ray diffraction allowed to attribute the first endotherm (around -15°C) to $L\alpha$ -HII DOPE phase transition and the second one (around +30°C) to solid-liquid OA phase transition.

3.5. DOPE-OA-CHOL-ON mixtures

Finally, the effect of oligonucleotides on the thermal phase behaviour of a DOPE-OA-CHOL system (1:1.3:0.4 molar ratio) was investigated. The presence of a high concentration of oligonucleotide (0.02 ON/DOPE molar ratio) induced a high increase in DOPE transition temperature and a decrease in the transition enthalpy (Fig. 5A). In the case of a lower oligonucleotide concentration, the modifications were less pronounced: appearance of a small endotherm at -13.6°C and a slight decrease in total enthalpy corresponding to DOPE phase transition regions.

In the absence of ON, the X-ray patterns of DOPE-OA-CHOL, at -6°C, showed reflections in the ratios 1 (66.14), 1/√2 (46.19), 1/√3 (38.08), 1/2 (32.72), 1/√8 (23.71), indicating the presence of a cubic phase (in parentheses, measured values) (Fig. 5B). In contrast, the sample containing the lowest oligonucleotide concentration (0.002 ON/DOPE molar ratio) revealed the presence of two series of two X-ray spacings in the ratios of 1/1, 1/2, at the temperatures of -29, -15 and -6°C (Fig. 5C). These X-ray patterns suggested the existence of gel and liquid-crystalline lamellar phases of DOPE. At



43°C, however, X-ray lines which were observed in the ratios of 1, $1/\sqrt{3}$, $1/\sqrt{4}$ for both samples, characterize a hexagonal phase.

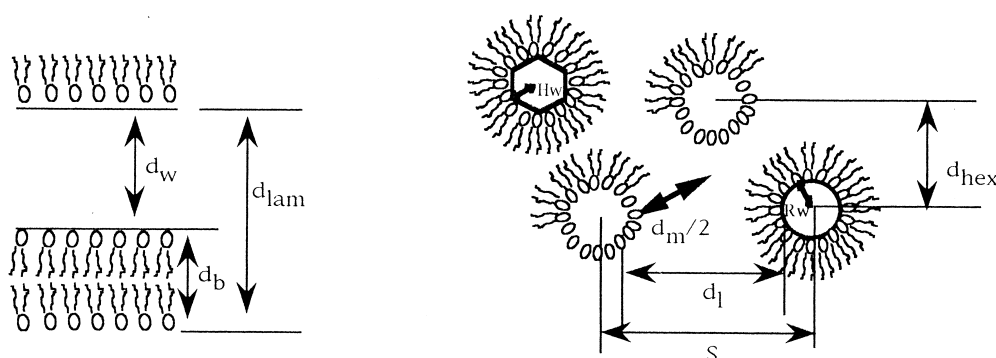
Fig. 5. Thermal phase behaviour of an oligonucleotide-containing DOPE-OA-CHOL system (1:1.3:0.4 molar ratio) (A). The calorimetric traces are shown in the absence (a) and in the presence of low ON concentration (0.002 ON/DOPE molar ratio) (b) and high ON concentration (0.02 ON/DOPE molar ratio) (c). Arrows show the temperatures at which X-ray patterns (B,C) were obtained. X-Ray diffraction patterns are those of a DOPE-OA-CHOL system (1:1.3:0.4 molar ratio) in the absence (B) and in the presence (C) of oligonucleotide (0.002 ON/DOPE molar ratio).

4. Discussion

PE are known to have a strong tendency to adopt the inverted hexagonal phase. At low water contents, this has been explained by the formation of phosphate-ammonium hydrogen bonds resulting in a decrease in the effective hydrophilicity of phosphatidylethanolamine headgroups [15]. Such intermolecular bonds are all the more favoured as the water content is low. Indeed, when hydrogen bonds can no more be satisfied with water, intermolecular bondings appear. The presence of a hexagonal phase in the case of our DOPE samples even at low temperatures, is then in good agreement with those reported in other studies [17–19], describing hexagonal phases in low hydrated DOPE samples.

The structural dimensions of the phase observed before and after phase transition by X-ray diffraction allowed to determine their crystalline parameters. According to Rand and Fuller [18], the water core prisms can be assumed either as circular in cross-section and of radius R_w , or as hexagonal in cross-section and of side H_w (Fig. 6). The reductions of the 'interaxial' 'bilayer' thickness, d_l , and of the interstitial length, d_m , observed for DOPE after the main transition at -11°C (Table 1) are consistent with the chain-ordered (or solid) hexagonal to chain-disordered (or liquid) hexagonal transition.

The presence of OA induced the appearance of a phase separation, resulting in domains with heterogeneous distribution of DOPE and OA, which is identified by the splitting of the DOPE transition peak in Fig. 1A. Furthermore, hydrogen bonding between PE molecules must be prevented by the presence of OA, and the interactions between hydrocarbon chains must be lowered. This can explain that DOPE transition shifted to lower temperatures in the



V_l = volume of one phospholipid molecule

V_w = volume of water per phospholipid molecule

ϕ_l = volume fraction of the non-aqueous part of the sample =

$$\frac{V_l}{V_l + V_w}$$

$d_b = \phi_l d_{lam}$

$d_w = d_{lam} - d_b$

$$R_w^2 = \frac{2d_{hex}^2(1-\phi_l)}{\pi\sqrt{3}}$$

$$d_l = s - 2R_w$$

$$d_m = 2 \left(\frac{s}{\sqrt{3}} - R_w \right)$$

$$s = \frac{2d_{hex}}{\sqrt{3}}$$

Fig. 6. Structural parameters describing molecular packing of the hexagonal and lamellar phases (according to [18]).

presence of OA. The calculated dimensions d_l and d_m (Table 1) support this interpretation since they are both increased by the presence of OA. The heterogeneous distribution of OA in itself can be attested by the presence of a lamellar OA phase melting around 30°C as indicated by both DSC and X-ray patterns (endotherm at 30°C and decrease in the spacing lines between 5.4 and 43.4°C).

The addition of ON molecules to DOPE, on the contrary, seemed to increase intermolecular interactions as evidenced by the increase in DOPE phase transition temperature. We can reasonably assume that phosphate groups brought by ON molecules participate in electrostatic interactions with PE amine headgroups, competing with PE phosphate's own groups. As regards structural dimension calculations (Table 1), ON favoured the ordered hexagonal phase by decreasing d_l and d_m , thus bringing PE molecules closer to each other. This can be explained by charge screening or intermolecular interaction which change the apparent v/al of DOPE as observed with ionic surfactants species [20]. Indeed, a curvature increase, corresponding to an increase in v/al ,

induces a decrease in both rod diameters and distances. Similar observations were found with DOPE/DOTAP cationic liposomes [21] in which DNA was shown to favour highly ordered structures.

Although bearing the same electric charge, it must be noticed, at this time, that OA and ON have opposite effects on v/al (likely due to the fact that one is amphiphilic and the other is not), which might compete when OA and ON would both be mixed with DOPE. Results described just before clearly showed that ON displaced OA from the lipid phase, as attested by the disappearance of peak splitting of DOPE transition and the increase in the enthalpy measured for the endotherm around 30°C, attributed to OA phase. These observations suggest that ON-DOPE interactions are stronger than OA-DOPE ones. This can easily be understood if we consider the length of ON molecules (15-mer) including 15 phosphate groups able to interact with amine DOPE headgroups. As proposed in Fig. 7, ON molecules might organize perpendicular to DOPE molecules, modifying the surface pressure. This model could explain the appearance of a lamellar phase

for DOPE in the presence of both OA and ON at very low temperatures (Fig. 4B), considering that ON might have increased lateral pressure in the DOPE headgroup region. Above the melting temperature (at -13.4°C), fluidity allows OA to leave the DOPE region and to gather in an extra lamellar phase. The absence of OA between DOPE molecules would then allow DOPE molecules to be brought closer to each other, favouring hexagonal phase formation (as illustrated in Fig. 7).

Concerning the endothermic event corresponding to buffer salts, OA and ON both tend to increase the temperature of this peak as shown for OA in Fig. 1A. This effect probably results from electrostatic interactions between OA or ON and the buffer components (carboxylic and phosphate groups on one hand, and Tris on the other hand).

Cholesterol is known to modify lipid fluidity and to decrease transition enthalpy of phosphatidylcholine derivatives. With both saturated or unsaturated phosphatidylethanolamines, a decrease in both melting enthalpies and temperature is observed as found by Van Dijck et al. [22], Takahashi et al. [23] and Blume [24]. In our study, cholesterol induced a temperature decrease in DOPE transition which is in good agreement with the literature. However, when OA is mixed with DOPE samples (1.3 and 2.4 molar ratio), it is interesting to note that the addition of cholesterol led to the co-crystallization of the lipids,

which was seen from the disappearance of the splitting of the transition peak of DOPE. As discussed above, this broad transition at lower temperature can be explained by taking into account DOPE intermolecular hydrogen bonds. Cholesterol, as OA, very likely interferes with the formation of these hydrogen bonds. Concerning samples containing both cholesterol and ON, it is interesting to point out that lamellar phases could be observed in a larger range of temperatures than in the absence of cholesterol. As described above, cholesterol may help the co-crystallization of lipids, and at least part of OA will be able to stay in DOPE regions above the solid/liquid transition. At higher temperatures, hexagonal transition occurs, leading to the clear appearance of OA lamellar phases (Fig. 5C, 43°C).

This study clearly demonstrated that interactions between ON and DOPE occur when molecules are in close contact. Because of the number of electrostatic interactions able to form between one ON molecule and DOPE, the interactions of ON with liposomal membrane are rather strong (able to displace OA molecules). In the presence of OA and cholesterol, they are strong enough to favour a lamellar phase over a large range of temperatures. In our study, whereas OA alone could not allow the formation of lamellar phase, ON supplied the default of water and satisfied hydrogen bonds with DOPE. Such a result would let think that the phase behaviour of pH-sensitive liposomes in the endosomal compartment could be altered by the presence of ON. However, in these conditions, water molecules will be in large excess, and will compete with ON. In order to clarify the comportment of pH-sensitive formulations in a biological medium, studies in fully hydrated systems are currently in progress in our laboratory.

Acknowledgements

We thank the Fundação Coordenação de Aperfeiçoamento de Pessoal de Nível Superior-CAPES, Brazil, for supporting Mônica Cristina De Oliveira with a scholarship. We also thank the GDR from the CNRS No. 1207 for financial support. We thank G. Keller (URA CNRS 1218) for his technical support.

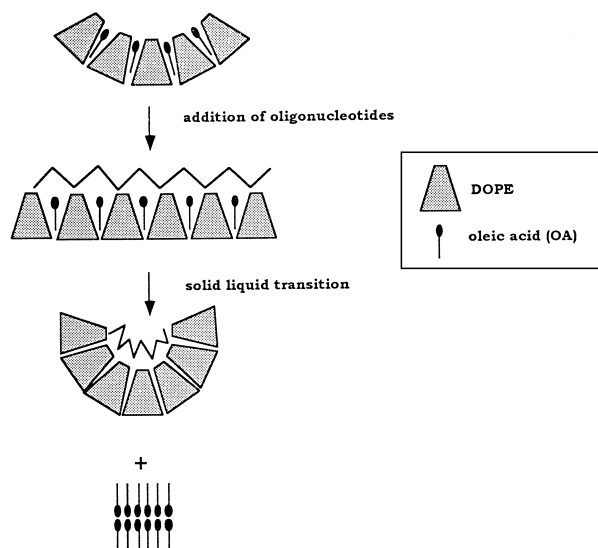


Fig. 7. Schematic representation of the interactions likely to occur between oligonucleotides and DOPE in the presence of OA.

References

- [1] C.-Y. Wang, L. Huang, *Biochemistry* 28 (1989) 9508–9514.
- [2] C.-J. Chu, J. Dijkstra, M.-Z. Lai, K. Hong, F.C. Szoka, *Pharm. Res.* 7 (1990) 824–834.
- [3] R. Reedy, F. Zhou, L. Huang, F. Carbone, M. Bevan, B.T. Rouse, *J. Immunol. Methods* 141 (1991) 157–163.
- [4] M.-J. Choi, H.-S. Han, H. Kim, *J. Biochem.* 112 (1992) 694–699.
- [5] D.C. Litzinger, L. Huang, *Biochim. Biophys. Acta* 1113 (1992) 201–227.
- [6] K. Kono, K.-i. Zenitani, T. Takagishi, *Biochim. Biophys. Acta* 1193 (1994) 1–9.
- [7] X. Zhou, A.L. Klibanov, L. Huang, *J. Liposome Res.* 2 (1992) 125–139.
- [8] H. Ellens, J. Bentz, F.C. Szoka, *Biochemistry* 23 (1984) 1532–1538.
- [9] M.B. Yatvin, W. Krentz, M. Horwitz, M. Shinitzky, *Science* 210 (1980) 1253–1255.
- [10] D. Liu, L. Huang, *Biochim. Biophys. Acta* 1022 (1990) 348–354.
- [11] D. Collins, D.C. Litzinger, L. Huang, *Biochim. Biophys. Acta* 1025 (1990) 234–242.
- [12] J.M. Seddon, *Biochim. Biophys. Acta* 1031 (1990) 1–69.
- [13] C. Ropert, M. Lavignon, C. Dubernet, P. Couvreur, C. Malvy, *Biochem. Biophys. Res. Commun.* 183 (1992) 879–885.
- [14] C. Ropert, C. Malvy, P. Couvreur, *Pharm. Res.* 10 (1993) 1427–1433.
- [15] C. Ropert, Z. Mishal, J.M. Rodrigues, C. Malvy, P. Couvreur, *Biochim. Biophys. Acta* 1310 (1996) 53–59.
- [16] G. Keller, F. Lavigne, C. Loisel, M. Ollivon, C. Bourgaux, *J. Therm. Anal.* 47 (1996) 1545–1565.
- [17] K. Gawrisch, V.A. Parsegian, *Biochemistry* 31 (1992) 2856–2864.
- [18] R.P. Rand, N.L. Fuller, *Biophys. J.* 66 (1994) 2127–2138.
- [19] M.M. Kozlov, S. Leikin, R.P. Rand, *Biophys. J.* 67 (1994) 1603–1611.
- [20] J.N. Israelachvili, D.J. Mitchell, B.N. Ninham, *J. Chem. Soc. Faraday Trans. 2* (1976) 1525–1567.
- [21] J.O. Rädler, J. Koltover, T. Salditt, C.R. Safinya, *Science* 275 (1997) 810–814.
- [22] P.W.M. Van Dijck, B. De Kruijff, L.L.M. Van Deenen, J. De Gier, R.A. Demel, *Biochim. Biophys. Acta* 455 (1976) 576–587.
- [23] H. Takahashi, K. Sinoda, I. Hatta, *Biochim. Biophys. Acta* 1289 (1996) 209–216.
- [24] A. Blume, *Biochemistry* 19 (1980) 4908–4913.